GEOPHYSICAL RESEARCH LETTERS, VOL. 34, L23807, doi:10.1029/2007GL031867, 2007

Click Here for Full Article

Tropical cyclone energy dispersion under vertical shears

Xuyang Ge,[1] Tim Li,[1,2] and Xiaqiong Zhou[1]

Received 29 August 2007; revised 7 October 2007; accepted 6 November 2007; published 7 December 2007.

[1] Tropical cyclone Rossby wave energy dispersion under easterly and westerly vertical shears is investigated in a baroclinic model. In a resting environment, the model simulates a Rossby wave train that has a baroclinic structure with alternating cyclonic-anticyclonic-cyclonic (anticyclonic-cyclonic-anticyclonic) circulations in the lower (upper) troposphere. A significant asymmetry appears in the wave train development under easterly and westerly vertical shears, that is, an easterly (westerly) shear confines the maximum amplitude of the wave train primarily to the lower (upper) level. It is proposed that the vertical wind shear may impact the Rossby wave train development through both the barotropic-baroclinic mode coupling and the modulation of the group velocity by the mean flow through a "Doppler shift effect". Additional experiments with uniform westerly and easterly mean flows confirm the hypothesis. The enhancement of the Rossby wave train in the lower level by the easterly shear may have an important implication for understanding the tropical cyclogenesis and the origin of the synoptic wave trains in the western North Pacific. **Citation:** Ge, X., T. Li, and X. Zhou (2007), Tropical cyclone energy dispersion under vertical shears, *Geophys. Res. Lett.*, *34*, L23807, doi:10.1029/2007GL031867.

1. Introduction

[2] Tropical cyclone (TC) Rossby wave energy dispersion in a barotropic dynamic framework has been studied in a great deal [e.g., *Anthes*, 1982; *Flierl*, 1984; *Chan and Williams*, 1987; *Luo*, 1994; *Carr and Elsberry*, 1995; *McDonald*, 1998]. While a TC moves northwestward due to mean flow steering and the planetary vorticity gradient, Rossby waves emit energy from the TC center southeastward. As a result, a synoptic-scale wave train with alternating anticyclonic and cyclonic vorticity perturbations forms in its wake. Using a non-divergent barotropic model, *Carr and Elsberry* [1995] noted that both the linear (beta term) and nonlinear (advection term) processes might determine the scale and the orientation of a Rossby wave train.

[3] TC energy dispersion (TCED) in a 3D dynamic framework was recently examined by *Ge et al.* [2007]. The result shows that the Rossby wave has a baroclinic structure, and there is a connection between the upper and lower tropospheric wave perturbations. However, this study examines the energy dispersion of a baroclinic TC under a resting environment. How and to what extent the environment flow modulates the wave train development is unclear. An observational study by *Li and Fu* [2006] reveals that for the western North Pacific (WNP) TCs, the Rossby wave trains are only observed west of 160°E where the mean easterly shear is pronounced. The easterly and westerly shear may have a significant effect on equatorial Rossby waves [*Wang and Xie*, 1996]. Thus it is important to explore how the vertical shear of the mean zonal flows impacts the growth and evolution characters of the Rossby wave train induced by TCED.

[4] The paper is organized as follows. In section 2, a brief description of the model and experimental design is given. This is followed by the presentation of the model simulation results and physical interpretation in section 3. The concluding remarks are given in section 4.

2. Model and Experiment Designs

[5] The model used here is a hydrostatic primitive equation model formulated in the Cartesian horizontal coordinates and σ (pressure normalized by the surface pressure) vertical coordinate. The details of the model description and its capability in simulating baroclinic TCs are documented by *Wang* [2001]. In this study, a 30 km horizontal resolution with 201 × 201 grid points centered at 18°N is applied. At this intermediate resolution, a mass flux convective parameterization scheme [*Tiedtke*, 1989] is used to calculate the effect of subgrid-scale cumulus convection. The initial axisymmetric vortex has a radial and vertical tangential wind profile as follows:

$$V_t = \begin{cases} \frac{3\sqrt{6}}{4} V_m \left(\frac{r}{r_m}\right)\left[1+\frac{1}{2}\left(\frac{r}{r_m}\right)^2\right]^{-\frac{3}{2}} \sin\left[\frac{\pi}{2}\left(\frac{\sigma-\sigma_u}{1-\sigma_u}\right)\right], & \sigma > \sigma_u; \\ 0 & \sigma \le \sigma_u; \end{cases}$$

where r is the radial distance from the vortex center, V_m the maximum tangential wind at the radius of r_m and $\sigma_u = 0.1$. Therefore, the initial cyclonic vortex has a maximum azimuthal wind of 30 ms^{-1} at a radius of 100 km at the surface, decreasing gradually to zero at about 100 hPa.

[6] Five experiments are designed. The first control experiment (CTRL) is designed to examine 3D energy dispersion in a quiescent environmental flow. To study the vertical shear effect, we conduct two constant vertical-shear experiments in which the zonal basic flow is only a linear function of height and does not change with the zonal and meridional directions. In the easterly (westerly) shear experiment, a shear strength of 10 ms^{-1} [i.e., linearly decreasing (increasing) of the zonal wind from 5 (−5) ms^{-1} at the surface to −5 (5) ms^{-1} at the top] is specified. To compare with the vertical shear experiments, two experiments with

[1]Department of Meteorology, University of Hawaii at Manoa, Honolulu, Hawaii, USA.
[2]International Pacific Research Center, Honolulu, Hawaii, USA.

Copyright 2007 by the American Geophysical Union.
0094-8276/07/2007GL031867$05.00

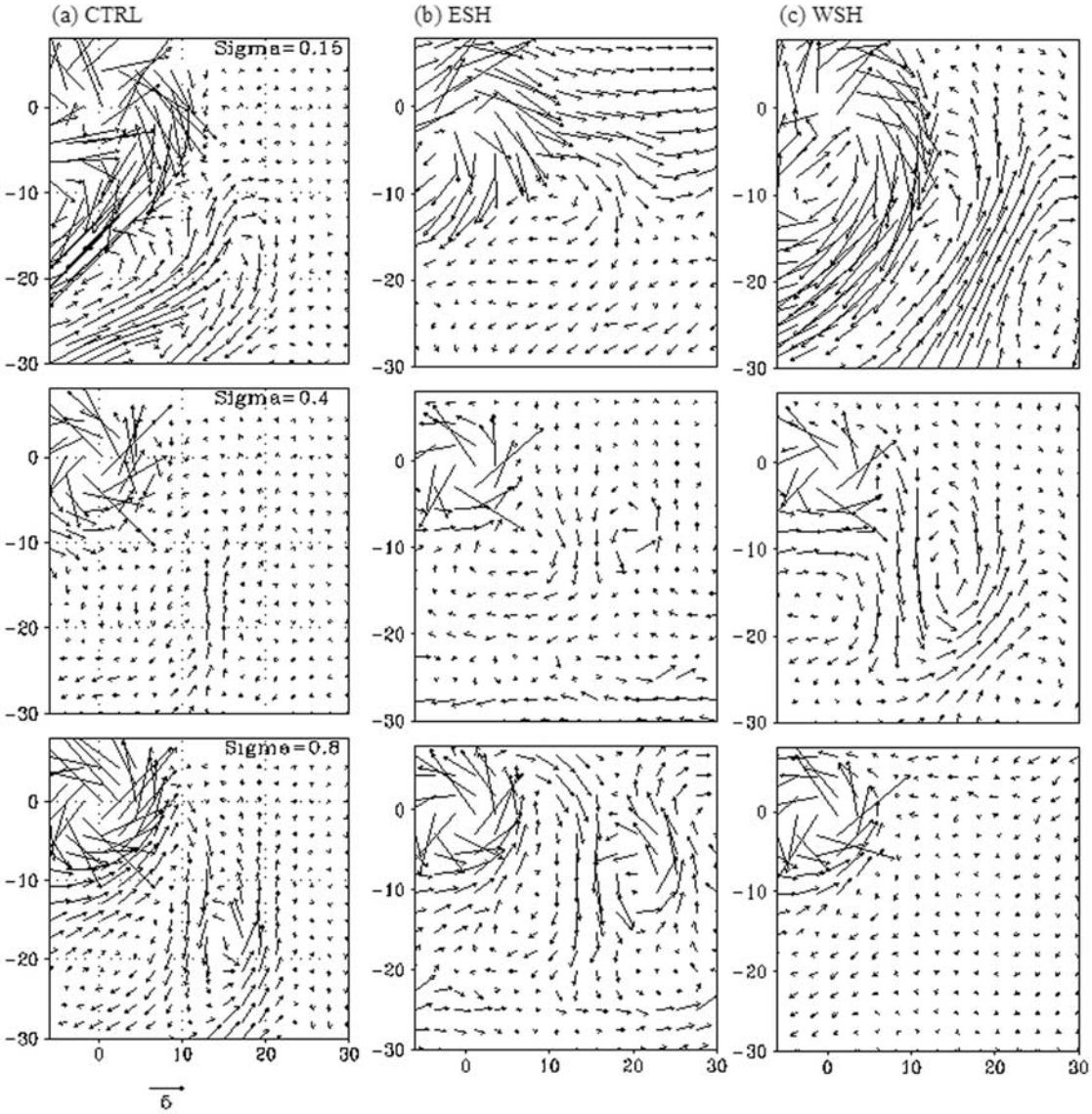

Figure 1. Wind fields in CTRL (left panel), ESH (middle panel) and WSH (right panel) at different sigma levels from the upper to lower level at day 7. The domain averaged mean flows at each level are removed in both WSH and ESH. The point (0, 0) represents the TC center. Horizontal distance has a unit of 100 km.

either an uniform mean westerly (W5) or easterly (E5) flow with a magnitude of 5 ms^{-1} are conducted, respectively.

3. Numerical Results

[7] In CTRL, the model is initialized with a TC-like vortex on a beta-plane in an environment at rest. The model TC moves northwestward due to the beta-effect induced "ventilation flow" advecting the core vortex. After a rapid intensification for a period of about 36 h, the model TC reaches a quasi-equilibrium state. Meanwhile, it is evident that the isobars are elongated westward, forming an elliptic outer structure. A weak wave train with alternating cyclonic-anticyclonic-cyclonic circulations starts to develop in the TC wake at day 5. The horizontal patterns of the TCED-induced Rossby wave train at different sigma level are presented in Figure 1a. The lower level pattern is quite similar to those retrieved from the QuikSCAT observations [*Li and Fu*, 2006]. The northwest-southeast orientated wave train has a wavelength of 2000–2500 kilometers. The wave trains appear clearly in both upper and lower troposphere, with the alternation of anticyclonic-cyclonic-anticyclonic (cyclonic-anticyclonic-cyclonic) circulation in the upper (lower) level. The amplitude of the wave train is minimum in the mid-troposphere. Moreover, the upper level wave train has larger amplitude but is shallower than the lower level counterpart. These features are attributed to the differential dynamic effect of inertial stability and stratification with elevation in a baroclinic TC [*Ge et al.*, 2007]. Figures 1b and 1c show the simulated Rossby wave train under easterly and westerly vertical shears. For better comparison with CTRL, the domain averaged mean flows at each level have

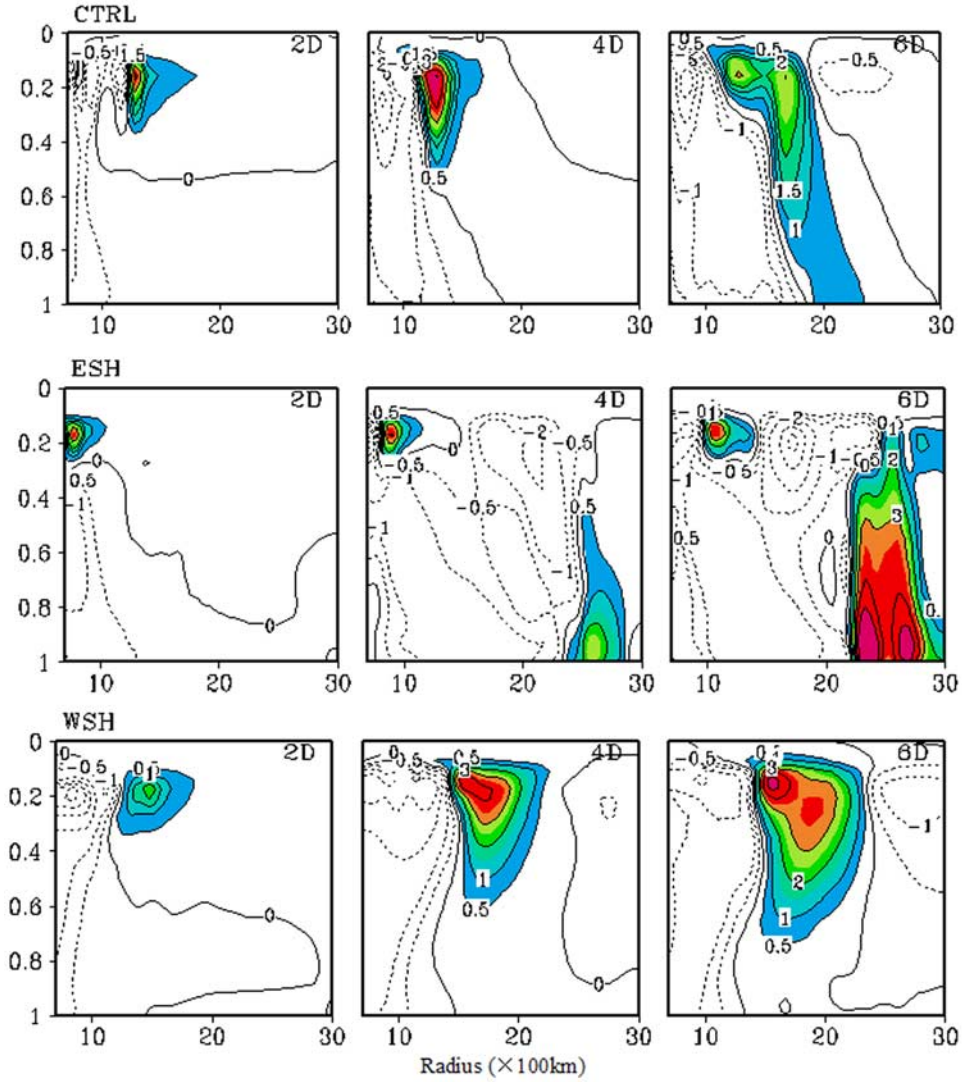

Figure 2. Time evolutions of the vertical-radius cross sections of relative vorticity (unit: $\times 10^{-5}$ s^{-1}) of CTRL (top panel), ESH (middle panel) and WSH (bottom panel) along the northwest-southeast oriented axis. The number in the upper-right of each panel indicates the time of day.

been removed. In the easterly wind shear (ESH) case, the lower level wave train is strengthened, whereas the upper level wave train weakens significantly. No obvious wave-like pattern is observed in the upper level. In a sharp contrast, in the westerly wind shear (WSH) case, the upper level wave train is significantly enhanced, while the lower level counterpart is hardly identified. The results show that TCED process is greatly modulated by the environmental flows.

[8] To further demonstrate the difference, we present the time evolutions of radius-vertical cross sections of relative vorticity along the axis of the wave train at the southeast quadrant (Figure 2). To highlight the wave train section, we only show the radial distance from 500 km to 3000 km. In CTRL, a positive relative vorticity perturbation initially develops in the upper troposphere ($\sigma = 0.15$), and thereafter intensifies and propagates both outward and downward. The region of relative vorticity greater than 0.5×10^{-5} s^{-1} (shaded area) reaches the planetary boundary layer (PBL) at day 6, coinciding with a cyclonic circulation center of the lower level wave train. A northwestward-tilting vorticity belt connects the upper and lower level wave trains. The northwestward-tilting vorticity belt appears in neither ESH nor WSH case. In WSH, a positive vorticity center occurs in the upper level first, and then penetrates into the middle level. However, it could not reach the lower level. In ESH, a positive vorticity center develops in the lower level at day 4, and this lower level development seems "disconnected" to the upper level vorticity center. The lower level cyclonic perturbation further enhances itself through the Ekman-pumping induced boundary layer convergence and through the moisture-convection-circulation feedback. As a result, the vorticity perturbation grows upward, which is different from a downward development in CTRL and WSH experiments.

[9] One possible cause of the downward-tilting development in CTRL is attributed to the differential inertial stability and beta-effect with elevation in a baroclinc TC

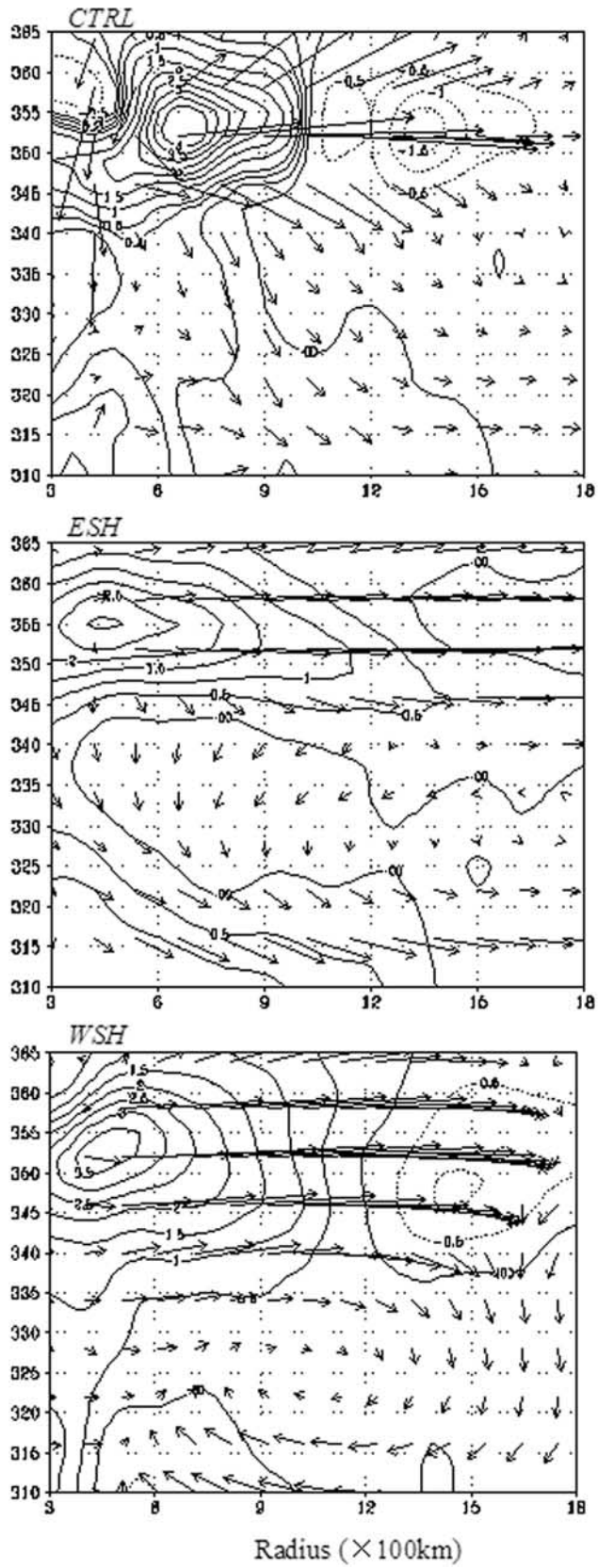

Figure 3. Potential temperature-radius cross sections of E-P flux vectors and their divergence (contour, unit: 0.5×10^4 Pa m^2 K^{-1} s^{-2}) for CTRL (top panel), ESH (middle) and WSH (bottom panel) at Day 4. The horizontal and vertical components are scaled by 1×10^{-9} and 1×10^{-5}, respectively.

[*Ge et al.*, 2007]. An upper (lower) level anticyclonic (cyclonic) circulation leads to weaker (stronger) inertial stabilities. As a result, the upper-level wave train develops much faster than these in the middle-lower levels. The slower responses in the lower levels may partially explain this downward development. Another possible mechanism is through the downward Rossby wave energy dispersion. Due to the lower inertial stability, the upper-tropospheric anticyclonic circulation rapidly induces an intense asymmetric outflow jet in the southeast quadrant, which further affects the lower level wave train through downward energy dispersion. To demonstrate this process, an E-P flux $\left(F \equiv \left[-r\overline{(\sigma u_L)'v_L'}, \overline{p'\frac{\partial\psi'}{\partial\lambda}}\right]\right)$ on a cylindrical coordinate is applied to illustrate the energy propagation of the Rossby waves [*Molinari et al.*, 1995; *Chen et al.*, 2003]. Figure 3 shows the radius-θ (potential temperature) cross sections of E-P flux vectors and their divergence ($\nabla \cdot F = -\frac{1}{r}\frac{\partial}{\partial r}r^2\overline{(\sigma u_L)'v_L'} + \frac{\partial}{\partial\theta}\overline{p'\frac{\partial\psi'}{\partial\lambda}}$) averaged at day 4. In all three experiments, the greatest eddy activities appear on the 355 K surface where the TC outflow jet is located. Note that the strong wave-mean flow interaction and large outward energy propagation occur in the upper outflow layer, which is consistent with the fast growth of the upper level wave train. In CTRL, along with the outward energy propagation, downward pointing vectors occur below the outflow layer (say θ = 355 k), indicating downward energy propagation. Both the outward and downward energy dispersion may account for the downward-tilting development as shown in Figure 2a. Of particular interest is an outward (inward) energy dispersion in the lower level in ESH (WSH), which is likely associated with the background mean flow.

[10] The stronger wave train responses in the lower (upper) level in ESH (WSH) are possibly attributed to the following two processes. The first is attributed to the interaction of baroclinic and barotropic Rossby modes in the presence of the background vertical shear. As shown in CTRL, the wave train exhibits the gravest baroclinic mode with an out-of-phase flow field in the upper and lower levels. In the presence of the vertical shear, a barotropic mode may be excited due to the baroclinic forcing. To verify this hypothesis, the barotrpoic components of three experiments are calculated. The result shows that the barotropic component of the wave train is significantly larger in both WSH and ESH than that in CTL (figure not shown). The baroclinic and barotropic modes are coupled in such a way that the two modes are nearly in phase in the westerly shear, whereas they are 180° out of phase in the easterly shear. Therefore, an easterly (westerly) shear leads to the amplification of the Rossby waves in the lower (upper) level [*Wang and Xie*, 1996]. The asymmetric responses in the wave train amplitude may be further strengthened by Ekman-pumping induced boundary layer moisture convergence through the circulation-convection feedback. The second process is likely attributed to the modulation of the Rossby wave group velocity by the background mean flow through a "Doppler shift effect". As a TC emits energy southeastward in both upper and lower levels in a resting environment, the mean westerly (easterly) flow may enhance (reduce) the total group velocity and thus accelerate (slow down) the wave train forma-

tion. Because of this group velocity modulation, the lower level Rossby wave train develops much slower and is suppressed in WSH compared to that in ESH.

[11] To understand the relative role of the two processes, we conduct two uniform mean flow (W5 and E5) experiments. To represent quantitatively the strength of the Rossby wave train, the lower level (σ = 0.8) relative vorticity averaged in an area of 1000 km $\times$ 1000 km (centered on the cyclonic circulation of the wave train, see the dotted line in Figure 4 for example) is listed in Table 1. Note that the lower level wave train is stronger in W5 than in E5 (Figure 4). Given that no vertical shear is presented in both the cases, the numerical experiments support the hypothesis that the westerly mean flow may enhance the group velocity and thus energy dispersion through the "Doppler shift effect". Of particular interest is that the strength of the lower level wave train is stronger (weaker) in ESH (WSH) than W5 (E5). This points out that the vertical shear further enhances the asymmetry in the wave train response. Therefore, the difference between these two sets of experiments gives rise to the "pure" vertical shear effect. Given that the difference in the wave train strength between W5 (6.1×10^{-6} s^{-1}) and ESH (12.6×10^{-6} s^{-1}) is 6.5×10^{-6} s^{-1}, which is much greater than the strength difference between E5 and W5. It is concluded that the vertical shear plays a greater role than the mean flow "Doppler" effect in causing the asymmetric wave train growth.

4. Conclusions

[12] In this study, the 3D tropical cyclone energy dispersion under various environmental flows is explored using a baroclinic model. Due to the differential inertial stability and beta effect with elevation, the simulated wave train exhibits a clear baroclinic structure with alternating anticyclonic-cyclonic-anticyclonic (cyclonic-anticyclonic-cyclonic) circulations in the upper (lower) level in an environment at rest. A remarkable asymmetry of the wave train growth appears in the presence of easterly and westerly vertical shears. An easterly (westerly) shear confines the maximum amplitude of the wave train to the lower (upper) level. It is suggested that the vertical shear may impact the Rossby wave train development through both the barotropic-baroclinic mode coupling and the modulation of the group velocity by the mean flow through a "Doppler shift effect". Under an easterly shear, a barotropic Rossby mode is generated in such a way that it enhances the lower level wave amplitude; meanwhile, the lower level westerly wind may accelerate the southeastward energy dispersion and strengthen the wave train strength. Both the processes favor the lower level Rossby wave train development. Once the lower level wave train is strengthened, it may reinforce itself through the Ekman-pumping induced PBL moisture convergence and the convection-circulation feedback.

[13] Further sensitivity experiments with two uniform mean flows confirm that both the vertical shear and the mean flow effects are important. A comparison of the wave train strength between the vertical shear and the uniform flow experiments indicate a greater role of the vertical shear in leading to the asymmetric wave train development. The enhancement of the Rossby wave train by background easterly vertical shears might have an important implication. During the boreal summer, significant easterly wind shears exist over the western North Pacific (WNP) monsoon region, thus providing a favorable large-scale environment for the Rossby wave train formation and development. The effect of the easterly wind shear on the tropical WNP cyclogenesis was emphasized recently by *Molinari et al.* [2007]. Therefore the current study may help understand the roles of TCED in the tropical cyclogenesis [*Holland*, 1995] and the origin of the summertime synoptic wave trains over the WNP [*Lau and Lau*, 1990; *Chang et al.*, 1996].

Table 1. Strength of the Lower Level Rossby Wave Train Represented By the Relative Vorticity Averaged Within the Cyclonic Circulation Region of the Wave Train at Day 7

Experiments	Mean Relative Vorticity, 10^{-6} s^{-1}
ESH	12.6
WSH	1.7
E5	4.3
W5	6.1

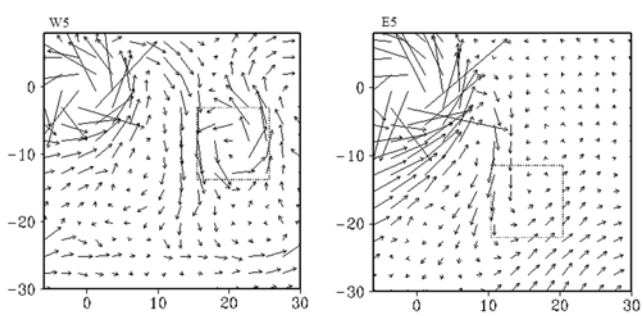

Figure 4. Wind fields in W5 (left panel) and E5 (right panel) at sigma = 0.8 level at day 7. The zonal mean flows at each level are removed. The dotted box denotes the cyclonic circulation region of the wave train being used to calculate the averaged relative vorticity to measure the wave train strength. Horizontal distance has a unit of 100 km.

[14] **Acknowledgments.** This work is supported by ONR grants N000140710145, N000140210532, and N001730619031. International Pacific Research Center is partially sponsored by the Japan Agency for Marine-Earth Science and Technology (JAMSTEC). This is SOEST contribution number 7217 and IPRC contribution number 485.

References

Anthes, R. A. (1982), Tropical cyclone: their evolution, structure and effects, *Meteorol. Monogr. Am. Meteorol. Soc.*, *41*, 208.

Carr, L. E., III, and R. L. Elsberry (1995), Monsoonal interactions leading to sadden tropical cyclone track changes, *Mon. Weather Rev.*, *123*, 265–289.

Chan, J. C. L., and R. T. Williams (1987), Analytical and numerical studies of the beta-effect in tropical cyclone motion, Part I: Zero mean flow, *J. Atmos. Sci.*, *44*, 1257–1265.

Chang, C.-P., J.-M. Chen, P. A. Harr, and L. E. Carr (1996), Northwestward-propagating wave patterns over the tropical western north Pacific during summer, *Mon. Weather Rev.*, *124*, 2245–2266.

Chen, Y. S., G. Brunet, and M. K. Yau (2003), Spiral bands in a simulated hurricane. Part II: Wave activity diagnostics, *J. Atmos. Sci.*, *60*, 1239–1256.

Flierl, G. R. (1984), Rossby wave radiation from a strongly nonlinear warm eddy, *J. Phys. Oceanogr.*, *14*, 47–58.

Ge, X. Y., T. Li, Y. Wang, and M. Peng (2007), Tropical cyclone energy dispersion in a three-dimensional primitive equation model: Upper tropospheric influence, *J. Atmos. Sci.*, in press.

Holland, G. J. (1995), Scale interaction in the Western Pacific monsoon, *Meteorol. Atmos. Phys.*, *56*, 57–79.

Lau, K. H., and N. C. Lau (1990), Observed structure and propagation characteristics of tropical summertime synoptic scale disturbances, *Mon. Weather Rev.*, *118*, 1888–1913.

Li, T., and B. Fu (2006), Tropical cyclogenesis associated with Rossby wave energy dispersion of a pre-existing typhoon. Part I: Satellite data analyses, *J. Atmos. Sci.*, *63*, 1377–1389.

Luo, Z. (1994), Effect of energy dispersion on the structure and motion of tropical cyclone, *Acta. Meteorol. Sinica*, *8*, 51–59.

McDonald, N. R. (1998), The decay of cyclonic eddies by Rossby wave radiation, *J. Fluid. Mech.*, *361*, 237–252.

Molinari, J., S. Skubis, and D. Vollaro (1995), External influences on hurricane intensity. Part III: Potential vorticity structure, *J. Atmos. Sci.*, *52*, 3593–3606.

Molinari, J., K. Lombardo, and D. Vollaro (2007), Tropical cyclogenesis within an Equatorial Rossby wave packet, *J. Atmos. Sci.*, *64*, 1301–1317.

Tiedtke, M. (1989), A comprehensive mass flux scheme for cumulus parameterization in large scale models, *Mon. Weather Rev.*, *117*, 1779–1800.

Wang, B., and X. Xie (1996), Low-frequency equatorial waves in sheared zonal flow, Part I: Stable waves, *J. Atmos. Sci.*, *53*, 449–467.

Wang, Y. (2001), An explicit simulation of tropical cyclones with a triply nested movable mesh primitive equation model: TCM3. Part I: Model description and control experiment, *Mon. Weather Rev.*, *129*, 1370–1394.

X. Ge, T. Li, and X. Zhou, Department of Meteorology, University of Hawaii, 2525 Correa Road, Honolulu, HI 96822, USA. (xuyang@hawaii.edu)